

**Exploring the Binding Free Energy Landscape of Intrinsically Disordered Protein-Protein
Interactions: Insights into the AF9-BCOR Complex implicated in Leukemia**

Shilpa Sharma and Arjun Saha*

Department of Chemistry and Biochemistry, University of Wisconsin-Milwaukee, Milwaukee,
Wisconsin, USA

*Email: saha6@uwm.edu

Supplementary Tables

Table S1: List of all the selected WT AF9-BCOR artificial complexes and their respective binding energies calculated from MM-GBSA analysis.

| S.No. | Complex Name | Avg. RMSD | Std. dev. | Avg. Rg | Std. dev. | Total interaction energy | Std. dev. | β-β interaction energy | Std. dev. |
|-------|--------------|-----------|-----------|---------|-----------|--------------------------|-----------|------------------------|-----------|
| 1 | 0-5 | 1.075 | 0.186 | 1.954 | 0.211 | -94.53 | 9.75 | -47.42 | 3.29 |
| 2 | 5-10 | 0.898 | 0.147 | 2.99 | 0.232 | -90.65 | 8.46 | -42.83 | 2.8 |
| 3 | 10-15 | 0.767 | 0.241 | 1.913 | 0.228 | -92.5 | 17.6 | -38.01 | 5.08 |
| 4 | 15-20 | 1.108 | 0.098 | 1.706 | 0.054 | -84.85 | 11.74 | -36.75 | 5.62 |
| 5 | 20-25 | 1.308 | 0.077 | 1.75 | 0.047 | -61.58 | 7.69 | -21.07 | 3.88 |
| 6 | 25-30 | 1.229 | 0.175 | 2.027 | 0.108 | -75.73 | 7.42 | -29.24 | 2.6 |
| 7 | 30-35 | 1.234 | 0.145 | 2.476 | 0.184 | -72.15 | 10.2 | -34.79 | 6.05 |
| 8 | 35-40 | 0.954 | 0.176 | 2.206 | 0.076 | -73.21 | 15.09 | -31.92 | 5.21 |
| 9 | 40-45 | 0.773 | 0.093 | 1.955 | 0.061 | -67.83 | 12.58 | -16.32 | 3.85 |
| 10 | 45-50 | 1.675 | 0.088 | 2.104 | 0.082 | -43.34 | 7.19 | -10.24 | 4.33 |
| 11 | 50-55 | 1.289 | 0.085 | 2.076 | 0.11 | -55.73 | 10.47 | -18.15 | 3.74 |
| 12 | 55-60 | 1.232 | 0.071 | 2.174 | 0.276 | -59.98 | 10.11 | -16.1 | 7.13 |
| 13 | 60-65 | 1.365 | 0.247 | 2.111 | 0.175 | -43.55 | 10.52 | -18.83 | 7.49 |
| 14 | 65-70 | 1.16 | 0.247 | 2.456 | 0.088 | -70.4 | 10.33 | -26.46 | 3.36 |
| 15 | 70-75 | 0.955 | 0.111 | 1.774 | 0.07 | -63.45 | 6.68 | -36.38 | 3.65 |
| 16 | 75-80 | 0.697 | 0.228 | 2.116 | 0.212 | -84.71 | 8.13 | -41.84 | 3.43 |
| 17 | 80-85 | 1.05 | 0.108 | 2.165 | 0.067 | -62.65 | 11.6 | -8.73 | 3.28 |
| 18 | 85-90 | 1.321 | 0.125 | 2.09 | 0.077 | -49.42 | 4.6 | -19.38 | 2.25 |
| 19 | 90-95 | 1.124 | 0.235 | 2.564 | 0.122 | -49.19 | 6.38 | -14.13 | 3.84 |
| 20 | 95-100 | 1.198 | 0.152 | 2.493 | 0.122 | -69.2 | 10.59 | -19.29 | 2.64 |
| 21 | 100-105 | 1.357 | 0.168 | 2.499 | 0.095 | -46.02 | 7.14 | -17.78 | 2.35 |
| 22 | 105-110 | 1.268 | 0.16 | 2.368 | 0.1 | -53.25 | 15.56 | -19.12 | 4.95 |
| 23 | 110-115 | 1.494 | 0.206 | 1.977 | 0.102 | -39.59 | 8.14 | -7.62 | 2.59 |
| 24 | 115-120 | 0.906 | 0.121 | 2.658 | 0.147 | -39.1 | 7.77 | -12.4 | 4.17 |
| 25 | 120-125 | 1.447 | 0.036 | 2.545 | 0.088 | -66.2 | 8.97 | -19 | 3.15 |
| 26 | 125-130 | 0.936 | 0.09 | 1.802 | 0.052 | -70.55 | 10.66 | -24.78 | 2.74 |
| 27 | 130-135 | 1.49 | 0.144 | 1.907 | 0.104 | -59.22 | 8.74 | -17.07 | 3.28 |

| | | | | | | | | | |
|----|---------|-------|-------|-------|-------|---------|-------|--------|------|
| 28 | 135-140 | 1.017 | 0.043 | 2.028 | 0.096 | -64.41 | 6.5 | -31.72 | 3.19 |
| 29 | 140-145 | 1.234 | 0.185 | 2.193 | 0.098 | -68.89 | 10 | -32.53 | 3.58 |
| 30 | 145-150 | 1.073 | 0.2 | 2.005 | 0.097 | -46 | 9.75 | -17.01 | 5.65 |
| 31 | 150-155 | 1.685 | 0.067 | 2.431 | 0.206 | -30.38 | 11.42 | -4.16 | 2.78 |
| 32 | 160-165 | 0.997 | 0.136 | 2 | 0.089 | -74.17 | 9.91 | -21.86 | 3.16 |
| 33 | 165-170 | 0.898 | 0.152 | 1.92 | 0.057 | -32.76 | 22.16 | 0.42 | 0.17 |
| 34 | 170-175 | 1.261 | 0.123 | 2.218 | 0.088 | -39.89 | 7.18 | -16.77 | 2.05 |
| 35 | 175-180 | 1.266 | 0.175 | 2.513 | 0.11 | -78.47 | 9.8 | -38.38 | 4.53 |
| 36 | 185-190 | 0.735 | 0.11 | 1.969 | 0.121 | -62.42 | 7.65 | -19.32 | 3.83 |
| 37 | 190-195 | 1.071 | 0.241 | 2.325 | 0.086 | -47.05 | 11.47 | -15.12 | 6.85 |
| 38 | 195-200 | 0.971 | 0.041 | 1.994 | 0.05 | -57.26 | 7.89 | -8.82 | 3.19 |
| 39 | A2B3 | 1.067 | 0.06 | 2.216 | 0.068 | -65.15 | 8.6 | -12.74 | 1.89 |
| 40 | A2B7 | 1.043 | 0.154 | 1.857 | 0.071 | -90.56 | 10.19 | -46.02 | 4.33 |
| 41 | A2B8 | 1.237 | 0.135 | 2.086 | 0.122 | -89.5 | 17.31 | -37.41 | 6.87 |
| 42 | A2B10 | 1.306 | 0.095 | 2 | 0.163 | -110.05 | 12.39 | -40.46 | 5.25 |
| 43 | A2B11 | 0.694 | 0.025 | 1.668 | 0.036 | -88.27 | 11.47 | -19.19 | 6.29 |
| 44 | A2B12 | 1.251 | 0.145 | 2.376 | 0.122 | -45.22 | 9.72 | -14.54 | 5.51 |
| 45 | A3B3 | 0.968 | 0.116 | 1.836 | 0.056 | -52.86 | 6.45 | -8.2 | 1.3 |
| 46 | A3B4 | 1.337 | 0.144 | 1.837 | 0.185 | -51.77 | 8.17 | -9.73 | 2.38 |
| 47 | A3B7 | 1.23 | 0.065 | 2.273 | 0.145 | -68.55 | 8.6 | -33.61 | 4.59 |
| 48 | A3B8 | 1.031 | 0.267 | 2.032 | 0.127 | -42.31 | 8.26 | -4.62 | 1.74 |
| 49 | A3B12 | 1.306 | 0.026 | 2.121 | 0.139 | -63.77 | 9.11 | -0.7 | 0.61 |
| 50 | A4B2 | 1.46 | 0.167 | 2.001 | 0.082 | -73.96 | 9.17 | -19.96 | 3.57 |
| 51 | A4B3 | 0.87 | 0.28 | 2.52 | 0.122 | -56.06 | 7.01 | -15.46 | 2.55 |
| 52 | A4B4 | 1.258 | 0.097 | 1.955 | 0.15 | -78.19 | 15.91 | -14.69 | 2.97 |
| 53 | A4B5 | 1.689 | 0.157 | 2.398 | 0.225 | -22.24 | 9.36 | -0.17 | 1.38 |
| 54 | A4B6 | 1.205 | 0.145 | 2.414 | 0.073 | -55.05 | 7.38 | -15.66 | 3.81 |
| 55 | A4B7 | 1.266 | 0.228 | 1.775 | 0.092 | -51.44 | 9.42 | -12.46 | 2.34 |
| 56 | A4B8 | 1.125 | 0.201 | 2.339 | 0.14 | -60.28 | 8.93 | -18.5 | 3.09 |
| 57 | A4B11 | 0.808 | 0.023 | 2.159 | 0.049 | -48.9 | 7.93 | -4.48 | 2.56 |
| 58 | A4B12 | 1.316 | 0.088 | 1.882 | 0.062 | -68.23 | 6.73 | -11.88 | 1.99 |
| 59 | A5B2 | 1.215 | 0.292 | 2.023 | 0.149 | -21.56 | 11.64 | -0.14 | 1.1 |
| 60 | A5B4 | 1.646 | 0.136 | 1.995 | 0.146 | -43.93 | 9.26 | -2.63 | 2.95 |
| 61 | A5B5 | 0.679 | 0.091 | 2.049 | 0.118 | -54.02 | 12.55 | -1.45 | 2.07 |
| 62 | A5B6 | 1.497 | 0.24 | 2.1 | 0.174 | -39.55 | 13.59 | -3.86 | 3.61 |
| 63 | A5B7 | 0.895 | 0.238 | 1.667 | 0.085 | -53.72 | 7.88 | -18.37 | 3.9 |
| 64 | A5B8 | 1.293 | 0.089 | 1.659 | 0.06 | -60 | 14.86 | -12.59 | 2.52 |
| 65 | A5B10 | 1.255 | 0.159 | 2.333 | 0.138 | -30.55 | 11.09 | -1.56 | 3.07 |
| 66 | A5B11 | 0.789 | 0.038 | 1.926 | 0.067 | -57.02 | 9.19 | 0.27 | 2.23 |
| 67 | A5B12 | 1.232 | 0.044 | 2.257 | 0.203 | -56.64 | 9.7 | 0.57 | 0.16 |
| 68 | A6B2 | 1.343 | 0.05 | 1.898 | 0.113 | -82.03 | 9.74 | -18 | 4.07 |
| 69 | A6B3 | 1.408 | 0.098 | 2.183 | 0.092 | -41.72 | 7.56 | -5.4 | 2.5 |
| 70 | A6B6 | 0.97 | 0.119 | 2.066 | 0.108 | -52.31 | 6.42 | -6.53 | 2.75 |
| 71 | A6B11 | 1.298 | 0.025 | 1.568 | 0.039 | -87.21 | 10.1 | -6.81 | 3.21 |
| 72 | A6B12 | 1.568 | 0.156 | 1.956 | 0.105 | -49.82 | 9.94 | -19.51 | 2.94 |

| | | | | | | | | | |
|-----|-------------|-------|-------|-------|-------|--------|-------|--------|------|
| 73 | A7B3 | 1.652 | 0.105 | 1.869 | 0.07 | -43.93 | 8.17 | -5.65 | 3.51 |
| 74 | A7B4 | 0.934 | 0.09 | 1.669 | 0.088 | -68.43 | 10.08 | -17.44 | 2.58 |
| 75 | A7B5 | 1.042 | 0.029 | 1.905 | 0.055 | -40.71 | 10.42 | 0.75 | 0.79 |
| 76 | A7B6 | 0.773 | 0.13 | 2.149 | 0.123 | -53.62 | 6.54 | -17.1 | 2.75 |
| 77 | A7B7 | 1.298 | 0.153 | 1.923 | 0.071 | -49.41 | 8.07 | -13.93 | 4.06 |
| 78 | A7B8 | 1.255 | 0.12 | 1.808 | 0.076 | -58.22 | 11.41 | -21.08 | 6.51 |
| 79 | A7B10 | 1.306 | 0.115 | 1.958 | 0.074 | -91.79 | 10.7 | -34.3 | 6.36 |
| 80 | A7B11 | 1.134 | 0.084 | 2.13 | 0.192 | -72.7 | 8.27 | -31.56 | 4.75 |
| 81 | A7B12 | 1.279 | 0.183 | 2.523 | 0.113 | -76.09 | 11.43 | -34.38 | 3.87 |
| 82 | A8B6 | 1.161 | 0.139 | 2.315 | 0.081 | -45.97 | 8.29 | -10.75 | 6.19 |
| 83 | A8B8 | 1.095 | 0.151 | 2.042 | 0.09 | -85.88 | 8.59 | -32.98 | 4.26 |
| 84 | A8B11 | 1.555 | 0.183 | 2.174 | 0.122 | -23.18 | 8.62 | -6.4 | 4.74 |
| 85 | A8B12 | 1.352 | 0.148 | 1.852 | 0.053 | -50.06 | 8.08 | -12.81 | 2.58 |
| 86 | A10B2 | 1.339 | 0.023 | 2.076 | 0.163 | -68.57 | 10.05 | -9.56 | 3.37 |
| 87 | A10B3 | 1.424 | 0.122 | 2.521 | 0.099 | -27.46 | 6.31 | -6.65 | 2.4 |
| 88 | A10B4 | 1.497 | 0.129 | 2.383 | 0.099 | -29.51 | 6.81 | -4.88 | 2.29 |
| 89 | A10B5 | 1.176 | 0.21 | 2.281 | 0.134 | -38.7 | 6.23 | -15.55 | 3.64 |
| 90 | A10B6 | 1.182 | 0.083 | 1.825 | 0.097 | -44.87 | 8.81 | -7.02 | 2.28 |
| 91 | A10B7 | 0.945 | 0.22 | 2.078 | 0.189 | -70.53 | 5.43 | -26.4 | 3.11 |
| 92 | A10B8 | 1.136 | 0.23 | 1.96 | 0.076 | -46.3 | 8.09 | -11.9 | 5.01 |
| 93 | A10B10 | 1.099 | 0.39 | 2.206 | 0.137 | -70.08 | 7.75 | -14.32 | 2.8 |
| 94 | A11B3 | 0.901 | 0.13 | 2.01 | 0.159 | -64.38 | 11.08 | -7.15 | 3.65 |
| 95 | A11B4 | 1.267 | 0.135 | 1.781 | 0.113 | -67.05 | 8.79 | -24.19 | 2.36 |
| 96 | A11B5 | 1.218 | 0.066 | 1.986 | 0.037 | -83.07 | 9.95 | -4.02 | 2.1 |
| 97 | A11B6 | 1.246 | 0.067 | 1.741 | 0.085 | -75.29 | 8.94 | -32.41 | 4.21 |
| 98 | A11B7 | 1.355 | 0.062 | 1.786 | 0.049 | -72.94 | 11.88 | -27.75 | 5.57 |
| 99 | A11B10 | 1.303 | 0.207 | 2.461 | 0.144 | -66.61 | 6.67 | -24.3 | 2.95 |
| 100 | A11B11 | 0.686 | 0.071 | 2.339 | 0.091 | -66.32 | 11.2 | -18.89 | 6.24 |
| 101 | A12B6 | 1.542 | 0.059 | 1.898 | 0.092 | -87.67 | 13.19 | -20.69 | 3.09 |
| 102 | A12B7 | 0.968 | 0.14 | 2.201 | 0.102 | -62.42 | 10.43 | -31.51 | 6.27 |
| 103 | A12B8 | 0.919 | 0.216 | 1.816 | 0.115 | -80.32 | 9.16 | -38.65 | 5.68 |
| 104 | A12B10 | 1.04 | 0.156 | 1.886 | 0.108 | -59.6 | 9.54 | -30.13 | 3.88 |
| 105 | A12B11 | 1.145 | 0.121 | 1.723 | 0.065 | -67.98 | 10.31 | -6.64 | 3.83 |
| 106 | A12B12 | 1.405 | 0.116 | 2.069 | 0.172 | -75.84 | 9.23 | -27.96 | 3.29 |
| 107 | WT (NMR) | 1.121 | 0.229 | 1.684 | 0.082 | -84.72 | 0.082 | -45.5 | 3.91 |

Table S2: List of all the MT AF9-BCOR artificial complexes and their respective binding energies calculated from MM-GBSA analysis.

| S.No. | Complex | Total Binding Energy | Std. dev. | $\beta\text{-}\beta$ interaction energy | Std. dev. |
|-------|---------|----------------------|-----------|---|-----------|
| 1 | 0-25 | -67.91 | 10.2 | -28.53 | 7.07 |
| 2 | 25-50 | -80.23 | 9.83 | -34.97 | 4.93 |
| 3 | 50-75 | -42.53 | 13.77 | -5.02 | 5.1 |
| 4 | 75-100 | -45.19 | 10.52 | -4.57 | 2.75 |
| 5 | 100-125 | -40.62 | 10.54 | -0.88 | 1.7 |
| 6 | 125-150 | -41.84 | 12.66 | -8.19 | 4.68 |
| 7 | 150-175 | -63.42 | 9.24 | -29.45 | 3.22 |
| 8 | 175-200 | -54.81 | 10.08 | -0.73 | 1.18 |

Supplementary Figures

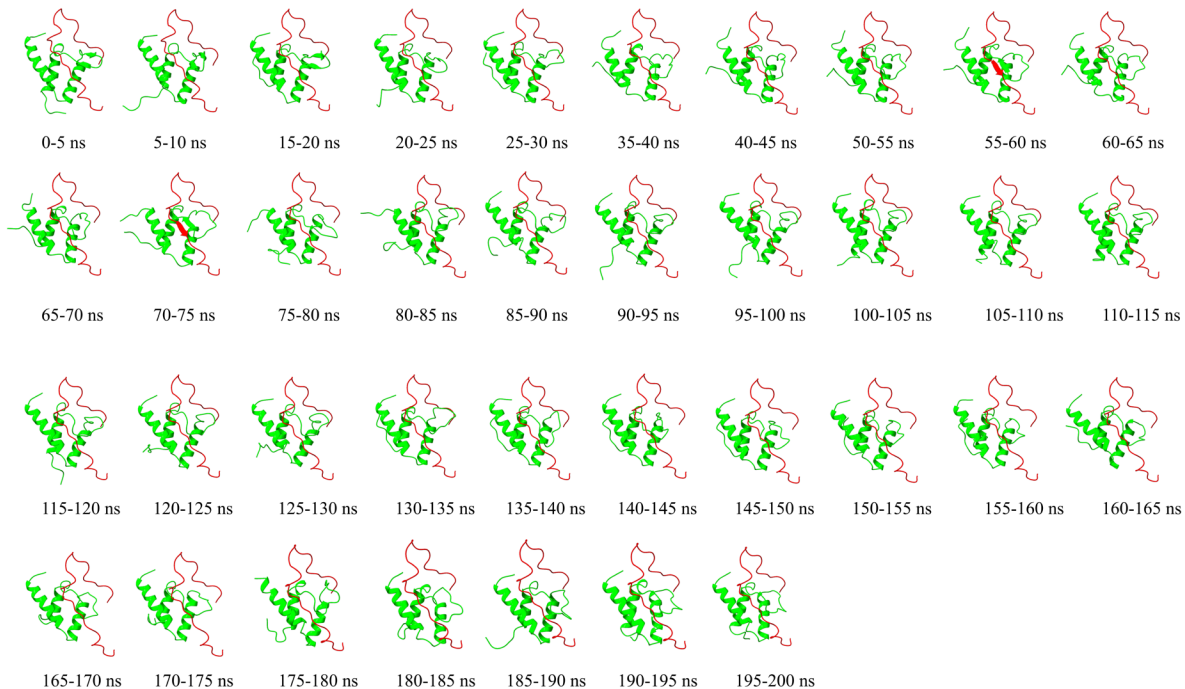


Figure S1: Initial structures of AF9-BCOR artificial complexes prepared through protocol 1.

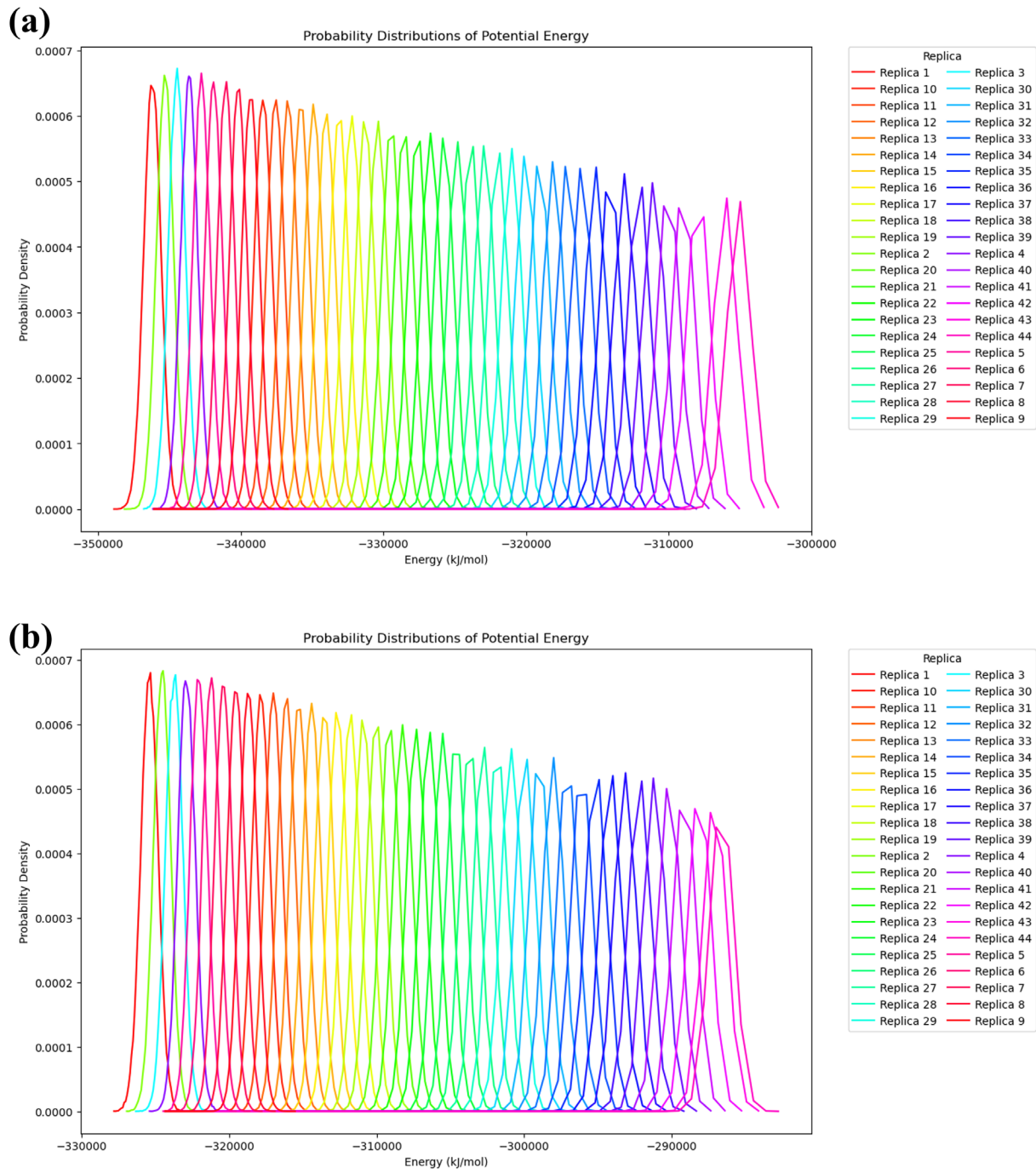


Figure S2: Monitoring the convergence of REMD simulations of (a) WT and (b) MT AF9 alone by checking the overlap of potential energy of all replicas.

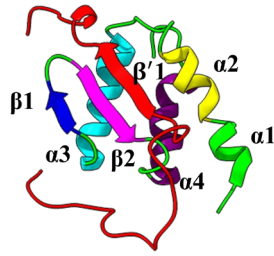


Figure S3: Labeled secondary structure components of AF9-BCOR complex.

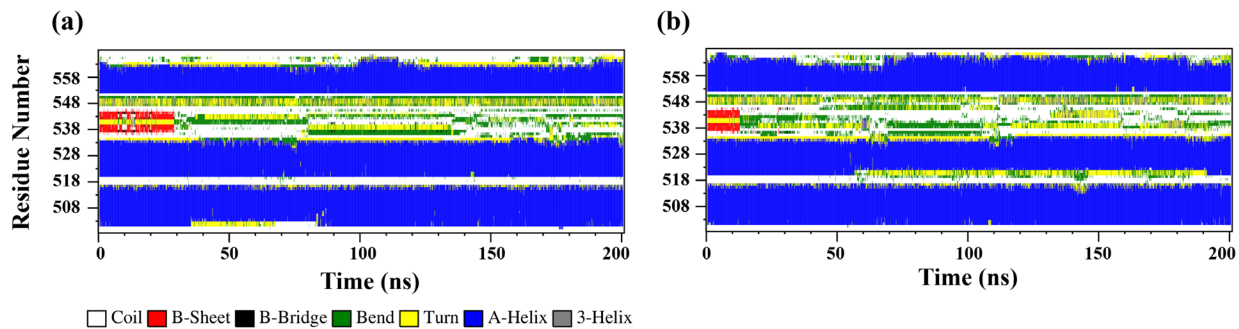


Figure S4: Secondary structure evolution of (a) WT AF9, and (b) MT AF9 with time. Various colors are used to represent different secondary structure components. α -helix, β -sheet, β -bridge, bend, turn, coil and 3-helix are shown in blue, red, black, green, yellow, white and grey, respectively.

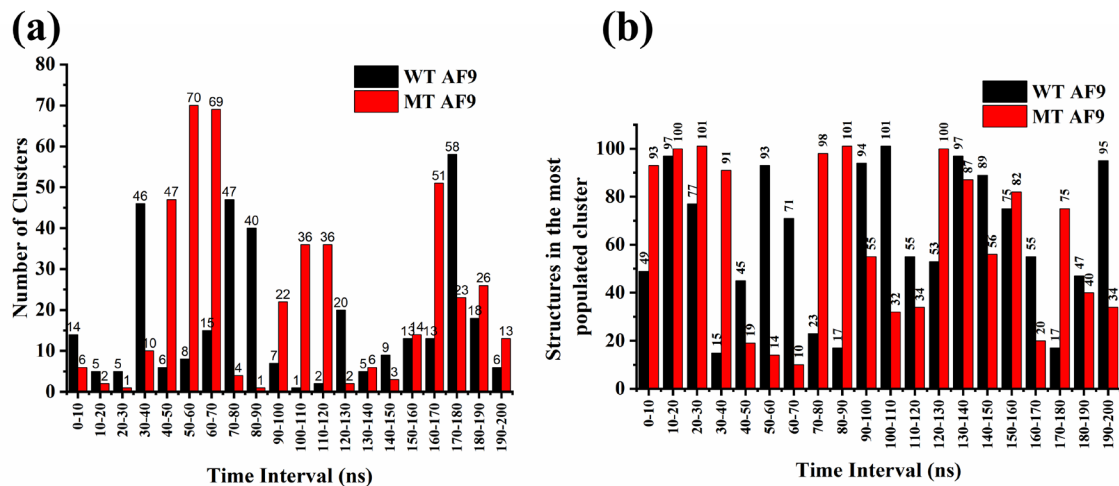


Figure S5: (a) Comparison of number of clusters and (b) total conformations present in the most populated cluster in WT and MT AF9.

Temperature Range: 303.15 – 450 K

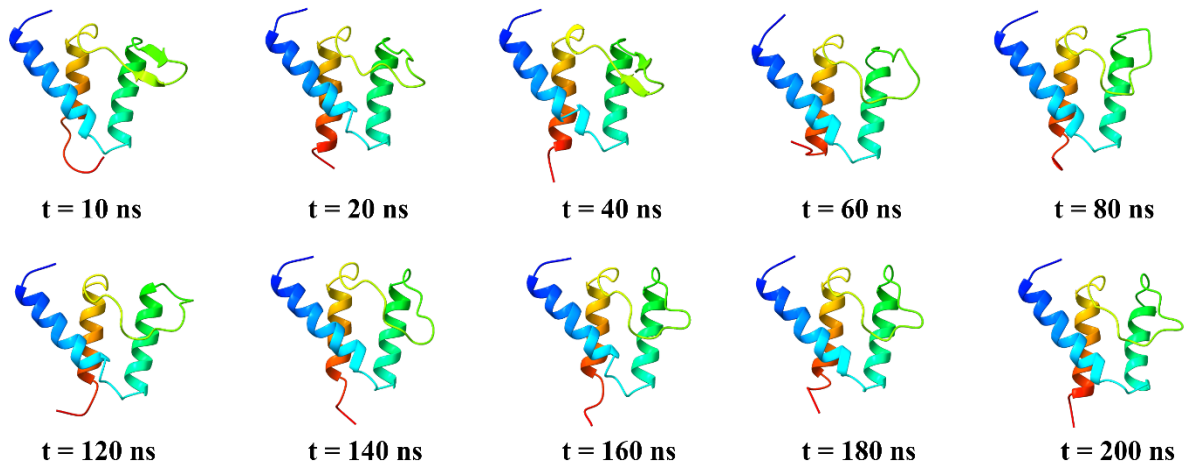


Figure S6: Conformations of WT AF9 obtained from the clustering analysis of REMD simulations performed at 303.15-450 K.

Temperature Range: 303.15 – 600 K

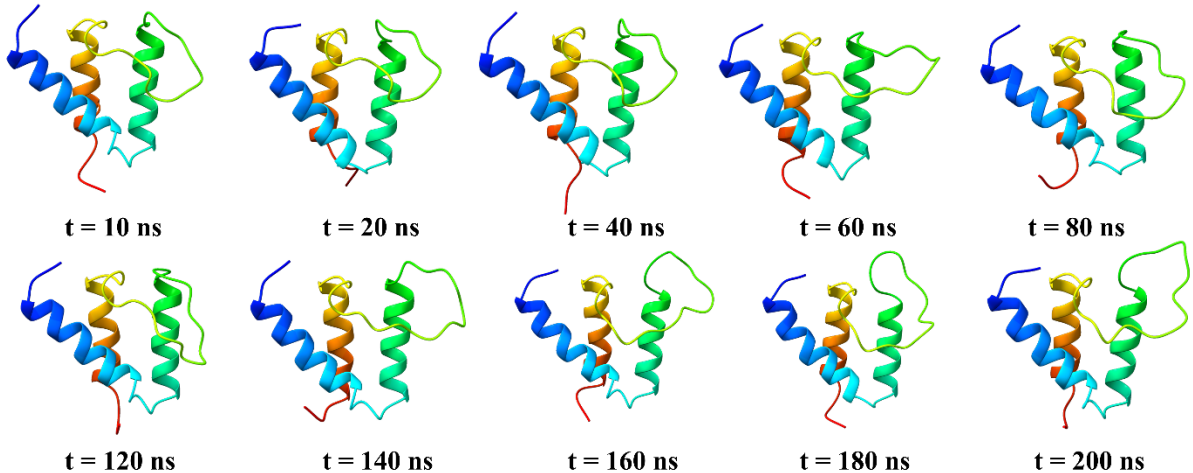


Figure S7: Conformations of WT AF9 obtained from the clustering analysis of REMD simulations performed at 303.15-600 K.

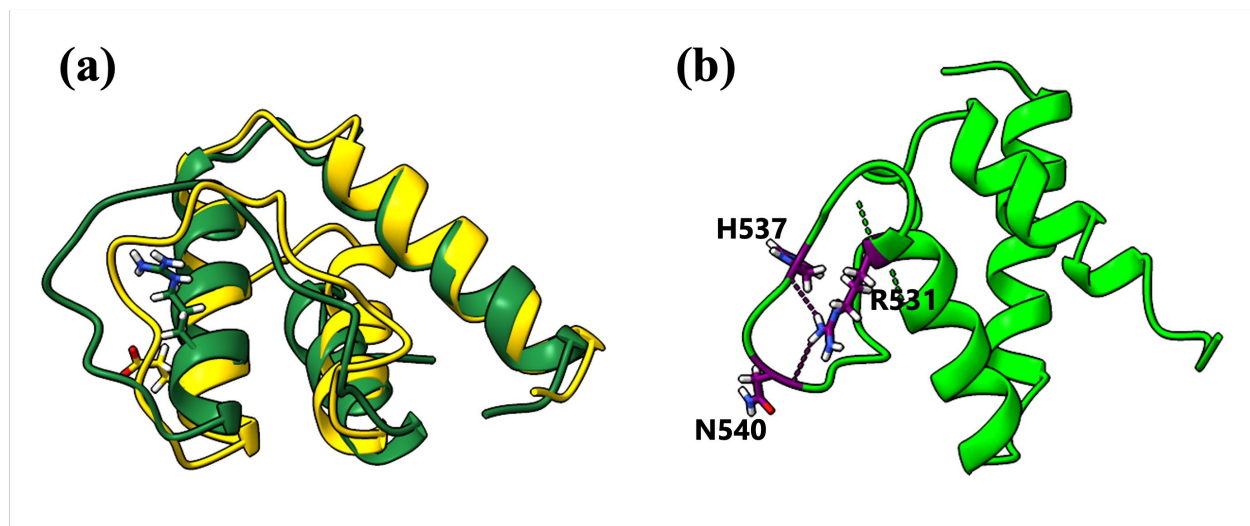


Figure S8: (a) The comparison of representative structures of WT and MT AF9. WT AF9 is shown in yellow color and MT AF9 is shown in green color. The mutated residue 531 is shown by sticks, (b) H-bonds formed between Arg531 and loop residues in MT AF9.

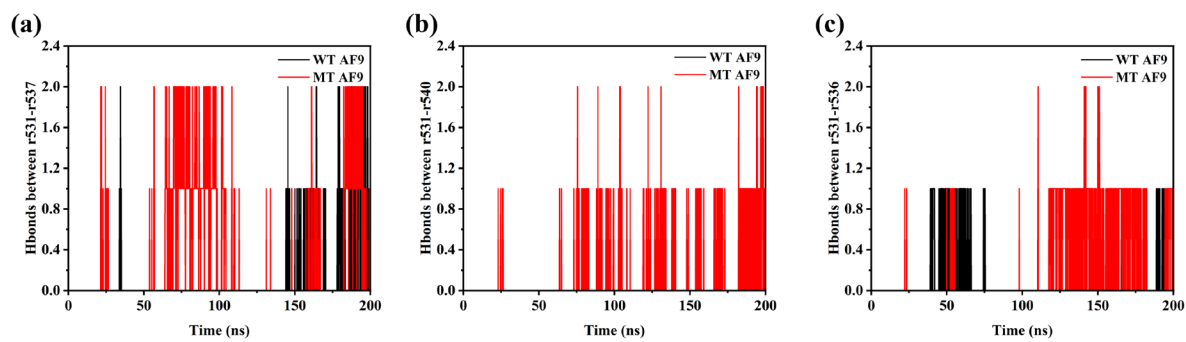


Figure S9: Intramolecular hydrogen bond formation between residue 531 and other residues (a) residue 537, (b) residue 540, and (c) residue 536 of AF9, before and after mutation.

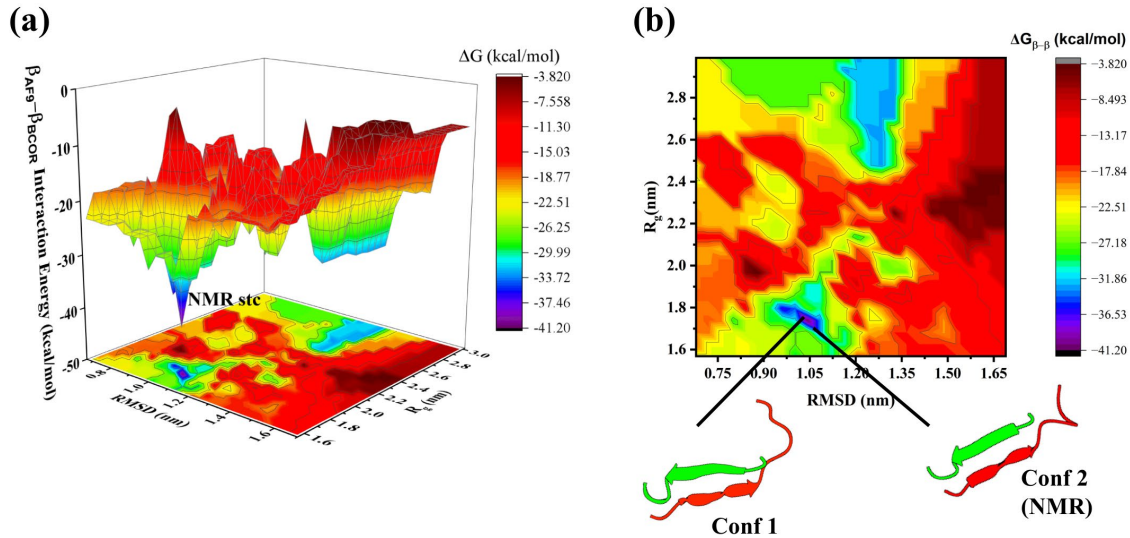


Figure S10: Binding free energy landscape (BFEL) of WT AF9-BCOR interaction constructed by calculating the $\beta_{\text{AF9}}-\beta_{\text{BCOR}}$ interaction energy of artificial complexes and NMR predicted complex (a) 3D BFEL and (b) 2D BFEL. The secondary structures of two minimum energy conformations (including experimental structure) obtained from the clustering of last 25 ns simulations, are shown by arrow.

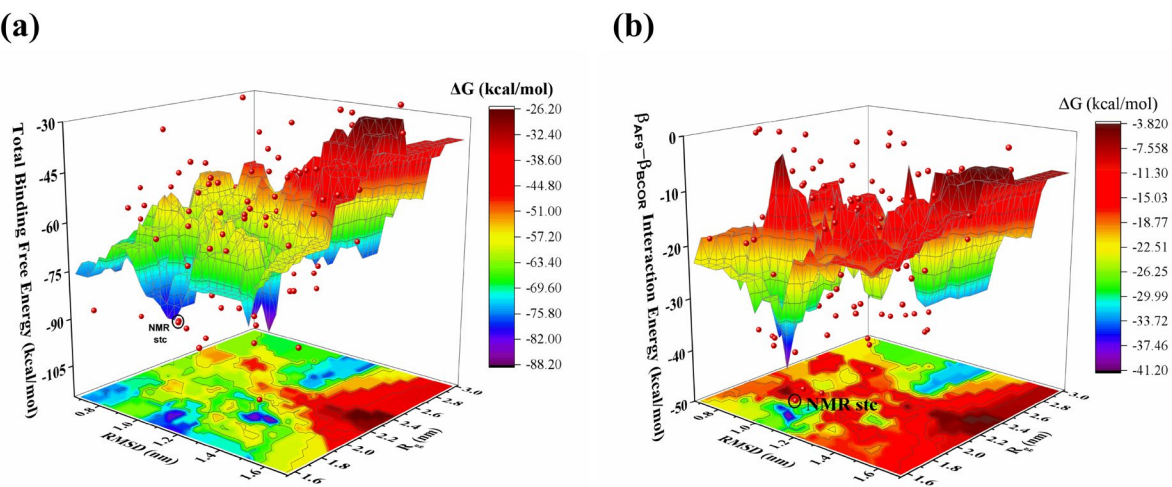


Figure S11: Binding free energy landscape (BFEL) of WT AF9-BCOR interaction constructed by calculating the (a) total binding free energy and (b) $\beta_{\text{AF9}}-\beta_{\text{BCOR}}$ interaction energy of artificial complexes and NMR predicted complex of WT AF9-BCOR. Raw data is shown by red spheres and energy surface was built through smoothening.

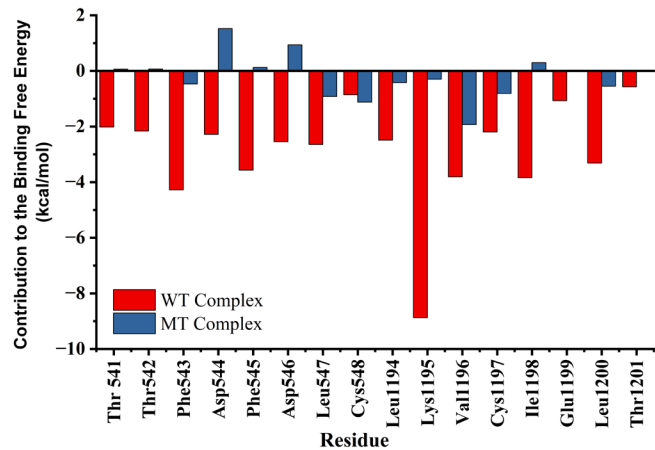


Figure S12: Per-residue contribution to the $\beta_{\text{AF9}}-\beta_{\text{BCOR}}$ binding free energy in WT and MT AF9-BCOR complexes.

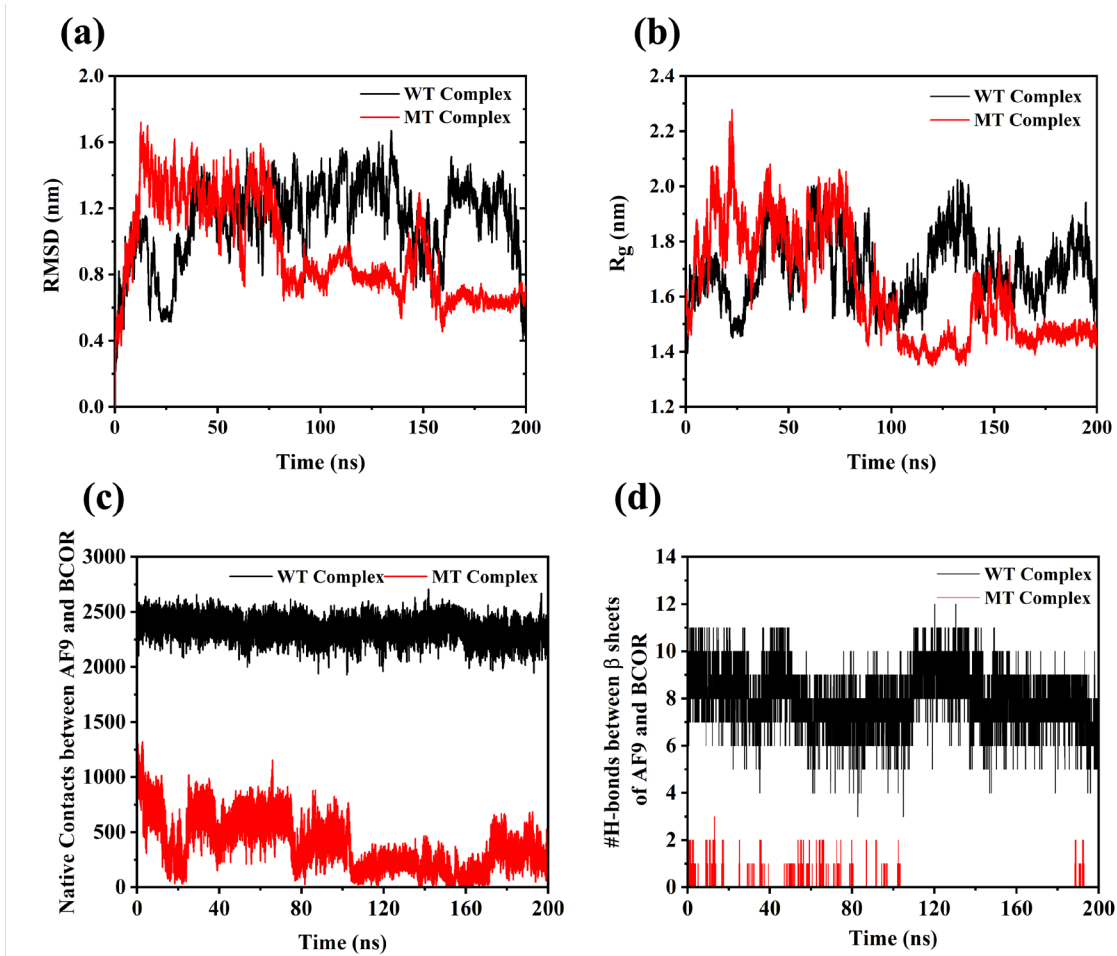


Figure S13: Comparison of structural properties of WT and MT AF9-BCOR complexes: (a) Ca root mean square deviation (RMSD) and (b) radius of gyration (R_g). Analysis of interaction

features: (c) native contacts between AF9 and BCOR, and (d) number of hydrogen bonds between AF9 and BCOR β -sheets.

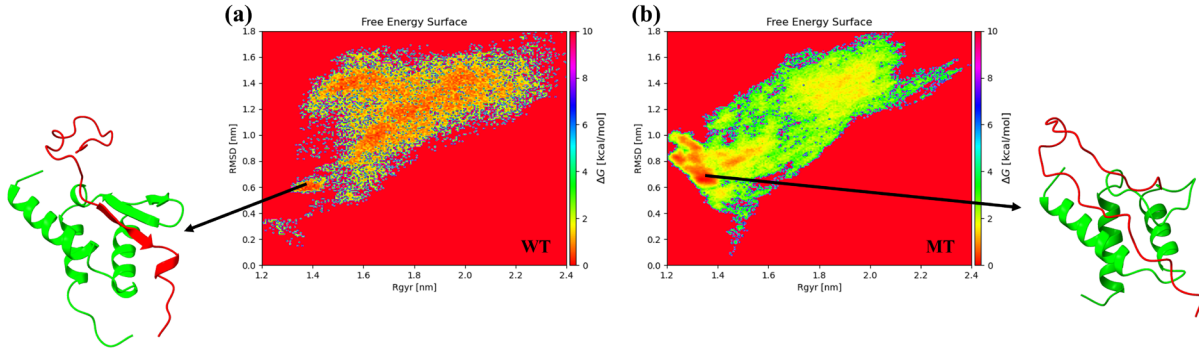


Figure S14: 2D free energy landscapes (FELs) of (a) WT, and (b) MT AF9-BCOR complexes. Black arrows indicate the minimum energy structure observed on the free energy surface, AF9 structure is shown in green and BCOR structure in red.

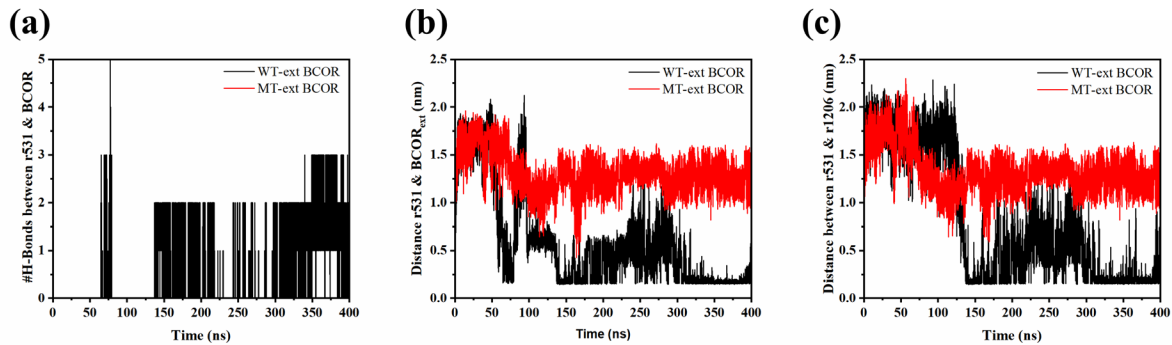
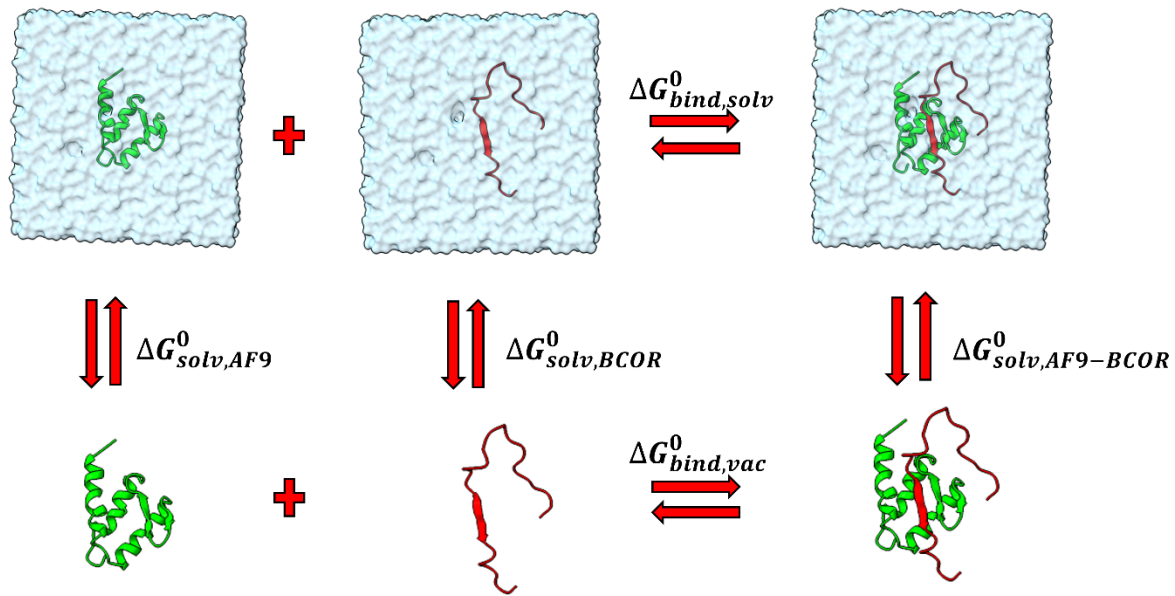


Figure S15: Monitoring the effect of mutation E531R on the interaction between AF9 and extended BCOR. (a) Number of H-bonds between residue 531 and BCOR_{ext}, (b) the distance between residue 531 and residue 1206-1226 of BCOR_{ext} and (c) distance between residue 531 and residue 1206.

Supplementary Schemes:



$$\Delta G_{bind,solv}^0 = \Delta G_{solv,AF9-BCOR}^0 + \Delta G_{bind,vac}^0 - \Delta G_{solv,AF9}^0 - \Delta G_{solv,BCOR}^0$$

$$\Delta G_{solv}^0 = \Delta G_{polar}^0 + \Delta G_{non-polar}^0$$

$$\Delta G_{bind,vac}^0 = \Delta E_{MM}^0 - T \Delta S^0$$

Scheme S1: Schematic representation of the thermodynamic cycle for the free energy calculation of AF9-BCOR using MM-GBSA method.